International Journal of
INTELLIGENT SYSTEMS AND APPLICATIONS IN ENGINEERING
ISSN:2147-6799 www.ijisae.org Original Research Paper

Model Reference Adaptive Controlled Bidirectional Battery Charger for EVs with Vehicle-to-Grid and grid-to-Vehicle Integration

[1]Mudassirhussain Mahammad, [2]Chandramouli Bethi

Submitted:07/02/2024 **Revised:**22/03/2024 **Accepted:**02/04/2024

Abstract: The development of efficient bidirectional battery chargers with both Vehicle-to-Grid (V2G) and Grid-to-Vehicle (G2V) capabilities is required because of the growing popularity of electric cars (EVs). This work presents a controlled bidirectional battery charging system that use an enhanced Marine optimization algorithm-based Model Reference Adaptive Controller (MRAC) to optimize regulation of the grid's and electric vehicles' electrical power flow. The proposed model is represented in MATLAB/Simulink 2021a, and the results show that assessed under different grid settings. Simulation findings validate that the system sustains balanced ensures dependable transitions among vehicle-to-grid (V2G) and grid-to-vehicle (G2V) operations, efficiently regulates the condition of charge (SOC) during battery charging and discharge, and displays three-phase voltage and current waveforms. The electrical voltage of the inverter as well as current waveforms demonstrate exceptional efficiency, characterized by few transients, hence facilitating smooth power flow. The findings confirm the practicality of using an adaptive control-based charging method to optimize energy use, promote stability of the grid, as well as make it easier to integrate modern smart grids with electric automobiles. Future enhancements may include real-time hardware deployment and incorporation of renewable energy sources to augment sustainability.

Keywords: *Vehicle-to-Grid (V2G), Grid-to-Vehicle (G2V), Bi-directional battery charger, Model Reference Adoptive Controller (MRAC), Electric Vehicle charging.*

1 Introduction

The rising reliance on traditional energy sources has led to environmental issues such as resource depletion and increased CO_2 emissions, contributing to global warming [1]. For more than a century, internal combustion engines (ICEs) have dominated the market, greatly increasing emissions and the use of fossil fuels. With solar power gaining traction due to its promise to lower emissions and lessen reliance on fossil fuels, this has expedited the worldwide transition to clean energy. By substituting electric propulsion systems for internal combustion engines (ICEs), the increasing popularity of electric cars (EVs) is also revolutionizing the transportation industry. New channels for energy flow in both directions between residences, automobiles, and solar-integrated grids are made possible by the combination of clean energy and electric cars [2]. A viable way to reduce emissions, use less oil, and fight climate change is via EVs. As manufacturing increases and battery prices decrease, EVs should become more affordable compared to traditional cars [3]. EV sales have risen from a specialist market to a mainstream choice over the last six years, reaching over two million units by early 2017 and making up more than 10% of new vehicle sales in a few of locations.

By providing affordable, clean power generated by the grid and other energy sources, strategically placed charging points for electric cars may hasten the widespread use of electric vehicles. [4]. By creating an appropriate network of charging stations, owners' concerns about

[1]*Research scholar, Department of EEE , Chaitanya deemed to be university, Himayathnagar , Moinabad, Hyderabad-500075.*

[2]*Professor , Department of EEE, Chaitanya deemed to be university, Himayathnagar, Moinabad, Hyderabad-500075.*

EVs will be reduced, enabling them to function comparable to engines with internal combustion [5]. Increasing the market penetration of electric vehicles is essential to highlight ongoing advancements in recharging technology. High-capacity batteries that function as onboard energy storage devices are a feature of EVs. These batteries provide the energy required to move the car forward by storing electricity. Longer driving ranges and more energy storage capacity are made possible by the ongoing improvements in battery capacities and energy densities brought forth by EV technology [6].

The growing adoption of EVs presents new technological and infrastructure challenges for existing power systems. As EV usage increases, so does electricity demand, especially during peak hours. At the same time, renewable energy sources like solar and wind remain intermittent, adding pressure on grid reliability. EVs, with their energy storage capability, can support two-way power flow systems through Vehicle-to-Grid (V2G) technology. Regulating both charging (G2V) and discharging (V2G) is essential for maintaining power quality. As more energy is stored in EV batteries, their interaction with the grid becomes a key feature of future autonomous energy systems.To enable the integration of clean energy and Plug-in Electric Vehicles (PEVs), smart grids focus on better coordination between distributed energy resources, energy storage, and grid operations. However, the variability of renewable sources presents challenges such as peak load management, load balancing, and reactive power support [7]. V2G-enabled PEVs can serve as prosumers, providing temporary power support via their energy storage systems (ESS) [8]. While rapid EV charging is essential, mass charging can lead to voltage drops, frequency issues, and increased total harmonic distortion (THD). These problems can be addressed through grid reinforcement or the use of renewables, although their intermittent nature requires effective storage solutions.

Smart grid initiatives are rapidly advancing worldwide [9], with EVs playing a key role as voltage sources that can support household loads through Grid-to-Vehicle (G2V), Vehicle-to-Grid (V2G), and Vehicle-to-Home (V2H) modes, especially in homes equipped with EV chargers (Figure 1).

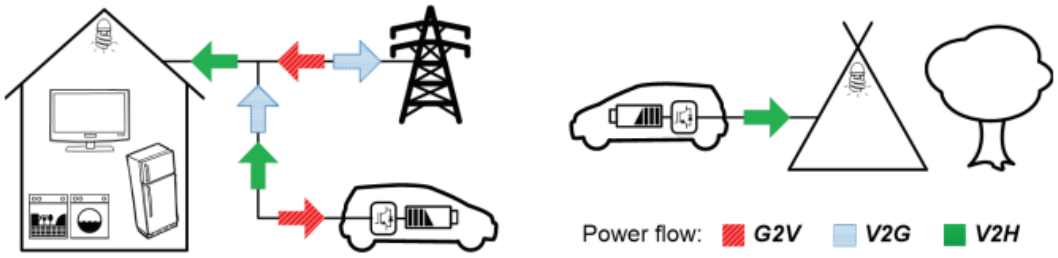

Figure 1 Concepts of the bidirectional battery charger with G2V, V2G and V2H technologies.

Bidirectional charging infrastructure is essential for enabling controlled two-way energy exchange between EVs and the grid. This capability supports grid stability by facilitating load balancing, peak shaving, and demand response management [10]. V2G systems also provide financial benefits to EV owners by allowing them to use stored energy during high-demand periods and sell surplus power back to the grid, reducing overall vehicle ownership costs [11].By supporting both charging and discharging, bidirectional charging improves battery performance and helps maintain grid reliability through frequency regulation and

energy optimization [12][13][14]. It enables off-peak charging for cost efficiency and leverages smart technologies to manage charging and discharging seamlessly.

The rise of PEVs offers sustainable benefits but also challenges like peak load stress, power quality issues, and battery wear. V2G technology addresses these by enabling bidirectional power flow, though current systems often lack real-time adaptability and efficient energy management. To address these gaps, this study proposes a hybrid control strategy using Model Reference Adaptive Control (MRAC) combined with an Improved Marine Optimization Algorithm (IMOA). While MRAC ensures accurate tracking and stability, IMOA enhances parameter tuning through dynamic optimization, improving energy efficiency and reducing battery stress. This approach supports smooth transitions across G2V, V2G, and V2H modes, promoting grid stability and EV sustainability.

2 Literature Review

Since energy management has an immediate effect on the effectiveness, range, and overall performance, it is an essential component of both its design and operation. It entails managing and maximizing the flow of energy among the several parts and systems, including the motor, battery, as well as regenerative brakes. To offer G2V and V2G/V2L capabilities, [15]incorporated a reversible charger with a multiport PV-assisted electric motor reconstruction. As a consequence, solar energy may be utilized to effectively charge EVs, and the grid may be powered by the EVs' batteries or other devices. Bi-directional charging, the electric vehicle battery charger's standout feature, has been discussed by [16]. The battery may be charged and drained at the same time thanks to this capability. Furthermore, it integrates technology such as G2V, V2G, and Vehicle-to-Load (V2L), can make it possible to utilize batteries effectively to provide power to houses or the grid when required. This innovative technology makes the charger more sustainable and versatile. [17]have spoken about V2G/G2V bidirectional charger topologies. These charging systems are able to utilize the batteries of EVs to return energy to the grid (Vehicle-to-Grid, or V2G) and charge EVs from the power grid (Grid-to-Vehicle, or G2V). This makes it easier to integrate EVs as a sustainable and adaptable resource into the electrical grid and permits efficient energy flow control.

Power generators, electric car chargers, and battery chargers might be controlled as supplementary power sources for electrical networks [18]. EVs may run in many modes and help the grid. The AIChOa maximizes the PI controller's gain. For electrical grid voltage THD, the recommended technique works better. Fast convergence and strong steady-state performance. According to [35], an EV charger's designed multiport converter is an effective method of converting solar energy to generate electricity for the vehicle. Furthermore, the charger may facilitate energy transfer from the electrical system to the vehicle, from the vehicle to the grid, and from PV to the vehicle since this converter allows energy to flow both ways. The real-time electricity cost model and internal battery costs were considered by the author of [19]to enable minimize costs for EV charging and discharging timing. [20] talks on how the spread of various PEVs affects various factors including grid security and power outages. The fact that only V2G or G2V modes are compatible with the PEV. is a major drawback of these investigations. For the best PEV charging scheduling, the authors in [21]offered a V2G/G2V charging strategy. However, the authors haven't been thoroughly investigated. Integration into the distribution grid requires

PEV charging coordination for two reasons. (i) financially rewarding PEV users who provide power to the grid using V2G mode; (ii) supporting grid load characteristics via G2V and V2G modes. Considering many objective functions, Considering a number of objective functions, the writers in [22] presented remedies for the problem of charge management. Although the investigations are not extensive, the authors of [23] presented the charging techniques by taking into account the load planning modes of G2V and V2G. In PEVs, aggregator coordinating charging (ACC) is crucial for cost reduction, load curve flattening, and user-driven charging scheduling depending on need and demand.

2.1 Research gap

Despite progress in V2G integration, existing control methods struggle with efficient energy transfer, system stability, and battery longevity. They lack real-time adaptability to dynamic grid conditions and are limited in handling nonlinearities and uncertainties, leading to slow convergence and inefficient parameter tuning. Moreover, most studies have not combined adaptive control with advanced optimization to simultaneously achieve fast response, optimal energy use, and extended battery life. This research addresses these gaps by introducing an MRAC tuned with IMOA, offering improved responsiveness, optimal parameter tuning, and enhanced performance for sustainable V2G applications.

3 Background

3.1 Power Electronic Charging Topology

It is projected that PEVs and their chargers will become more prevalent in the grid. It is crucial to have chargers and the advanced control systems that accompany them. components for making PEVs more competitive when compared to ICE cars because they enable the creation of ideal communication between the electrical system and the PEV. High power factor correction and reduced power loss are crucial for PEVs and charging stations to become a significant part of the electrical grid. Chargers and management systems enhance PEV competitiveness and facilitate connections between EV types, energy storage systems, and charging stations [24]. The charger's desired features are a power factor of one, reversible power capabilities (V2G and G2V), the ability to execute power management, little PQ effect, simplicity in structure as well as topology and suitability for a typical 16 A a single-phase plug [25]. This charger is suitable for domestic outlets due to its maximum power output of 2.3 kW. Power grid constraints and EU regulations define this power range.[26]. Figure 2's construction is based on the insulated gate bipolar transistor (IGBT). The IGBT is favored for its high efficiency and fast switching. In V2G mode, the AC-DC converter functions as an inverter, while in G2V mode, it acts as a rectifier. LC filters are used for energy storage and noise reduction. The C-class chopper performs buck conversion in G2V and boost conversion in V2G operation.

International Journal of
INTELLIGENT SYSTEMS AND APPLICATIONS IN ENGINEERING
ISSN:2147-6799 www.ijisae.org Original Research Paper

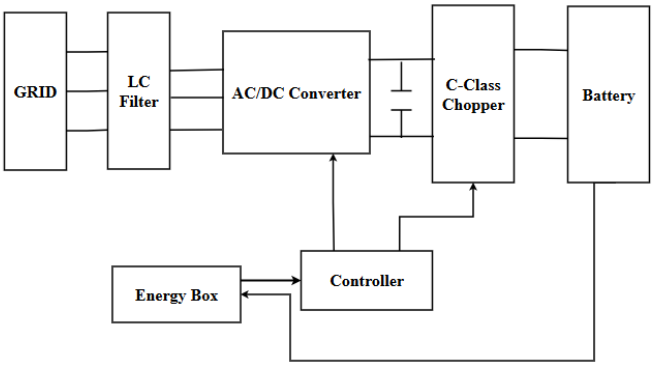

Figure 2PEV charger topology

DC/DC Converter Circuit Analysis

EVs batteries are charged using bidirectional type DC-DC converters (BDCs) using two stages: constant voltage mode and constant current mode. BDCs increase power density capacity by operating at high switching frequencies. Devices turning on and off quickly produce high-frequency noise, which damages other equipment linked to the grid and causes electromagnetic interference (EMI) inside the grid. Therefore, reliable EMI reduction and control techniques must be included into the design of BDCs.Because the DC/DC converter is a Class C chopper, it may operate in the first two quadrants, which include negative as well as positive flow and positive voltage. It is possible to synthesize the major operational equations using equations (1) to (4) for buck mode and (5) to (8) for boost mode.

$$V_{BAT} = V_{Cbus} - L_{Chopper} \cdot \frac{dI_L}{d_t} \quad (1)$$

$$I_L = \frac{1}{L_{Chopper}} \cdot \int_0^{Ton} \left(V_{VCbus} - V_{BAT}\right)\, dt \quad (2)$$

$$V_{BAT} = -L_{Chopper} \cdot \frac{dI_L}{dt} \quad (3)$$

$$I_L = \int_{Ton}^{Toff} \frac{V_{BAT}}{L_{Chopper}} dt \quad (4)$$

$$V_{BAT} = L_{Chopper} \cdot \frac{dI_L}{dt} \quad (5)$$

$$I_L = \frac{1}{L_{Chopper}} \cdot \int_0^{T_{on}} V_{BAT}^{\,dt} \quad (6)$$

$$V_{BAT} + V_{LChopper} = V_{Cbus} \quad (7)$$

$$I_L = \frac{1}{L_{Chopper}} . \int_{T_{on}}^{T_{off}} \left(V_{BAT} - V_{Cbus} \right) dt \qquad (8)$$

To control the ratio relationship between the chopper sides, a Pulse Width Modulation (PWM) signal may be used. For each power switch, the driving time (T_{on}) and cut-off time (T_s) make up a single switching period (T). Equations (9) and (10) for the buck mode and (11) and (12) for the boost mode explain the duty cycle (D), which determines the voltage conversion ratio of this circuit[27].

$$D = \frac{T_{on}}{T} \qquad (8)$$

$$V_{BAT} = V_{Cbus} . \frac{T_{on}}{T} = V_{bus} . D \qquad (9)$$

$$\frac{1}{1-D} = \frac{V_{Cbus}}{V_{BAT}} \Leftrightarrow D = -\frac{V_{BAT}}{V_{Cbus}} + 1 \qquad (10)$$

$$V_{BAT} = V_{Cbus} . \left(1 - D\right) \qquad (11)$$

Two essential parts for this converter's operation are the DC bus capacitor (C_{bus}) and the inductor (L Chopper). To determine the energy to be released for each chopper side (in buck or boost mode), the inductor works as an energy meter. It also helps control the ripple of the source current and mitigate the effects of high switching frequency . It is necessary to size the inductor according to the higher power level when the battery voltage is reduced, independent of the mode of operation. When using capacitor mode, equation (13) produces:

$$L_{Chopper} = \frac{V_{Cbus} - V_{BAT}}{2.\Delta I_L} \qquad (12)$$

$$DT = T_{on} \rightarrow \begin{cases} T_{on-} \min = \dfrac{V_{BAT_{\min}}}{V_{Cbus}} \cdot T \\ T_{on-} \max = \dfrac{V_{BAT_{\max}}}{V_{Cbus}} \cdot T \end{cases} \qquad (13)$$

AC/DC Converter Circuit Analysis

The proposed charger uses an AC/DC converter that acts as a rectifier in G2V mode to charge the battery and as an inverter in V2G mode to supply power back to the grid. Its use of low-resistance IGBT and unipolar PWM enhances efficiency and reduces voltage ripple. The PWM controller manages the operating mode and generates gate pulses for the converter.

3.2 Model Reference Adaptive Controller

Using the Model Reference Adaptive Controller block, discrete-time proportional-integral-derivative (PID) is used to achieve model reference adaptive control (MRAC). The controller, adjustment mechanism, and reference model for an MRAC system are its three primary parts (Figure.3).

International Journal of
INTELLIGENT SYSTEMS AND APPLICATIONS IN ENGINEERING
ISSN:2147-6799 www.ijisae.org Original Research Paper

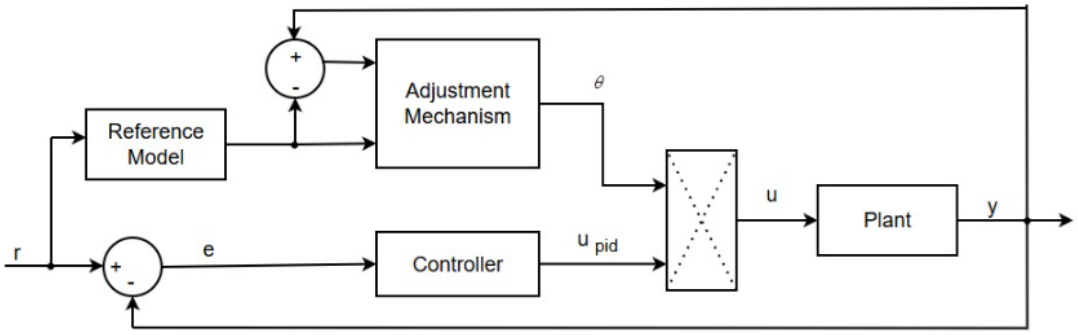

Figure 3 Block Diagram of Model Reference Adaptive Control (MRAC) System

The control equation is

$$u_{pid}(k)=\left[K_P+K_i\frac{T_{s^z}}{z-1}+K_d\frac{z-1}{T_{s^z}}\right]e(k), \quad (14)$$

Where, u_{pid} is the controller output, K_p is the proportional gain, K_i is the integral gain, K_d is the differential gain, T_s is the sample time, and e is the error.

The basis for the model is the closed-loop system's transmission function. The anticipated behavior of the a closed-l system is captured by this model. It is used as the transfer function in discrete time.

$$G_m(z)=\frac{B(z)}{A(z)} \quad (15)$$

Based on the discrepancy comparing the output of the facility to the benchmark model, the adaptation mechanism modifies the control action accordingly

$$\theta=(y-y_m)y_m\frac{-\gamma T_s z}{z-1}, (16)$$

Where, θ is the adaptation parameter, y is the plant output, y_m is the reference model output, and γ is the learning rate.

The quicker the plant adapts to changes, the higher the value of γ.

The modified signal for control, u, is

$$u(k)=u_{pid}(k)\theta(k) \quad (17)$$

3.3 Improved Marine Optimization Algorithm

IMO Algorithm extends the adaptability and effectiveness of MRAC with optimized control parameters for two-way battery charging in V2G applications. The algorithm realizes it through elite selection and dynamic foraging behavior

tactics, thus optimal adaptation under dynamically changing grid and battery environments.

Initialization and Search Agents

The IMO algorithm starts with an initial population of candidate solutions (search agents), represented as:

$$X = \{X_1, X_2, \ldots, X_N\} \quad (18)$$

where X_i represents the position (control parameter set) N is the total number of agents, and this is the case for the i-th search agent The search space is bounded by:

$$X_{\min} \le X_i \le X_{\max} \quad (19)$$

where $X_{\min}$ and $X_{\max}$ specify the top and lowest limits of the parameter search space.

Foraging-Based Movement Strategy

Marine predators use a combination of exploration (searching for new solutions) and exploitation (refining good solutions). The movement of agents is defined as:

$$X_i^{t+1} = X_i^t + r_1 \cdot \left(P_{best} - X_i^t\right) + r_2 \cdot \left(X_{elite} - X_i^t\right) \quad (20)$$

Where X_i^{t+1} is the updated position of the agent at iteration $t+1$, P_{best} is the best solution found so far, X_{elite} is the elite agent, and r_1, r_2 are random numbers in the range [0,1] that control stochastic movement.

Adaptive Convergence Control

To balance between local refinement (exploitation) and global search (exploration), an adaptive convergence factor α is introduced:

$$\alpha = \alpha_{\min} + \left(\alpha_{\max} - \alpha_{\min}\right) \times e^{-\beta t} \quad (21)$$

Where $\alpha_{\max}, \alpha_{\min}$ are the initial and final values of the convergence rate, β is the decay factor controlling the transition speed, and t is the current iteration.

Fitness Evaluation and Selection

Each agent's position is evaluated using an objective function $f\left(X_i\right)$, which optimizes voltage stability, reduced energy losses, and minimal battery degradation. The best-performing solutions are retained for the next generation:

$$X_{elite} = \arg\min f\left(X_i\right) \quad (22)$$

3.4 Updating MRAC Control Parameters

The IMO algorithm optimizes the adaptive gains K_p, K_i, K_d of the MRAC-based control for bidirectional charging:

$$U(t) = K_p e(t) + K_i \int e(t)\, dt + K_d \frac{d}{dt} e(t) \tag{23}$$

where $e(t)$ is the system error. The IMO algorithm ensures that these parameters are optimally tuned for faster convergence, stable charging dynamics, and lower grid harmonics.

3.5 ITAE as an Objective Function

The objective metric used to assess the system's performance is Integral of Time-weighted Absolute Error(ITAE). It reduces the component of the relative time-weighted error between the true and intended power output. The ITAE is responsible for the reduction of systemic errors, such as imbalances in energy supply and demand, over time, with a particular emphasis on errors that persist for extended periods. This facilitates the attainment of a more stable and fluid system performance.

4 Results

MATLAB Simulink 2021a is used to run the simulation. The system architecture and its simulation parameters are depicted in table 1 and figure 4. As it's shown in figure 4 the Plug-in-EV is connected to the utility through a wall charger connection box which contains Buck-Boost Converter, DC-DC Conversion with Battery Controller, DC-AC/AC-DC Converter, and Batteries Switching Control. As discussed in the methodology section the control action of battery controller is achieved using improved Marine optimization algorithm-based model reference adoptive controller. The designed control unit with model reference adoptive controller In Figure 5, the battery charger is seen.

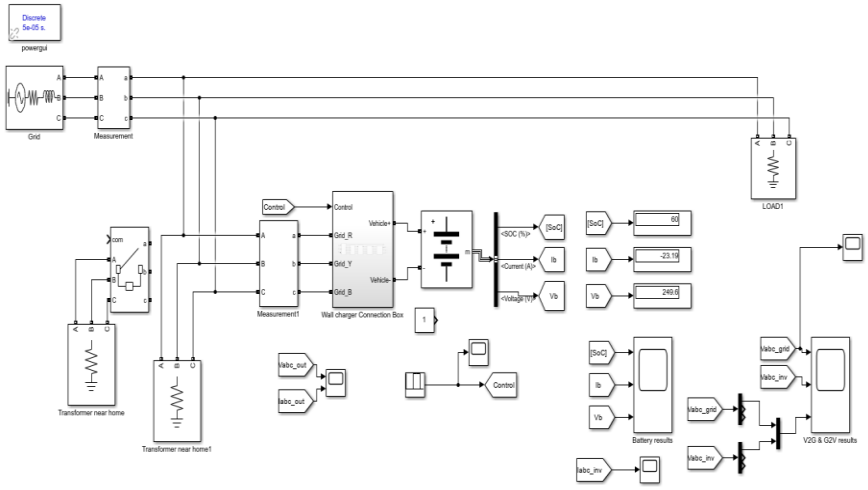

Figure 4 Design System architecture

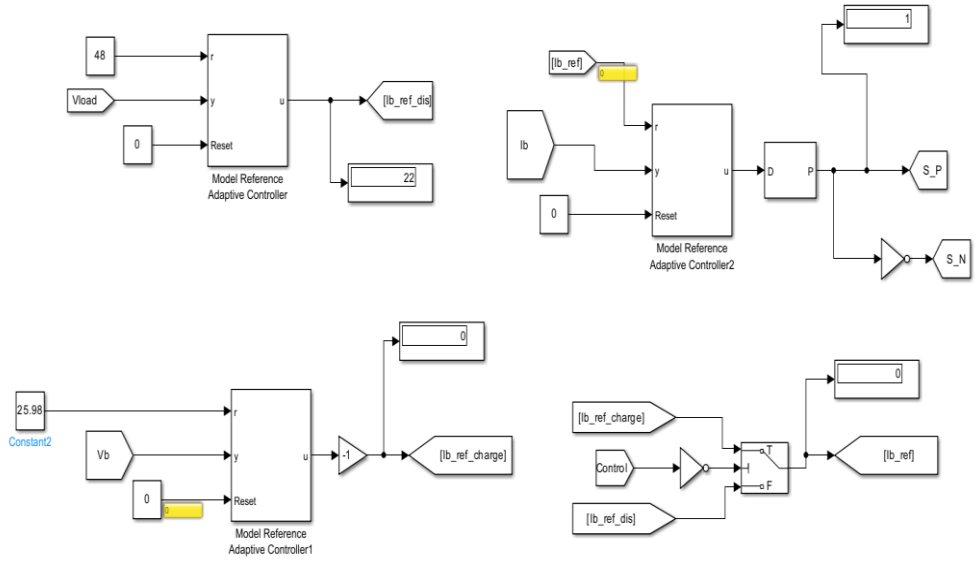

Figure 5 System design of Model Reference Adoptive Controller

The system architecture of MRAC used to control how a battery charges and discharges within a grid-connected energy management system. The figure has many MRAC blocks that modulate the reference current (Ib) according to input parameters, including voltage ($Vload, Vb$) and established setpoints. The top portion of the picture emphasizes the discharging process, whereby the controller interprets the input signals to produce a reference discharge current (Ib_ref_dis), which is then used for decision-making in the ensuing control blocks. The bottom part illustrates the charging control, whereby an additional MRAC block establishes the reference charging current (Ib_ref_charge) with a similar control methodology. Logical operations and control switches are included to regulate the transition between charging and discharging modes according to system circumstances. The architecture guarantees adaptive and optimal current regulation for efficient battery performance under fluctuating grid and load situations.

Table 1 Specifications and parameters of the system.

Network Components	**Parameter Values**
Load	Active Power(P): 1KW Nominal Phase-to Phase Voltage (Vn) = 380 V
Transformer	Delta (D1), Yg (Wye-grounded) 11 KV/ 0.4V, 20 KV/173 V R1=R2=0.003 p.u, L1=L2=0.08 p.u
Source	$V_{L\text{-}L}$=20kV, f=60Hz
Nominal frequency (Hz)	50
Active Power P (W)	20e3

Inductive reactive Power QL (positive var)	0
Capacitive reactive Power Qc (negative var)	0

4.1 Vehicle to Grid

The Vehicle Output Voltage and Currents (Figure 6) over a 0.5-second interval show balanced three-phase sinusoidal voltages (Va, Vb, Vc) at ±500 V, indicating a symmetrical system. The corresponding phase currents (Ia, Ib, Ic) oscillate around ±5000 A, reflecting load-dependent behavior and suggesting the use of high-frequency pulse-width modulation (PWM) for efficient power conversion.The Battery Performance (Figure 7) is illustrated through three plots: the State of Charge (SOC) declines steadily from 60%, indicating discharge; the battery current remains stable at approximately 22A; and the voltage slightly drops from 248V to 247V. These trends confirm consistent battery operation under continuous load conditions.The voltage and current behavior of the three-phase inverter system is analyzed through multiple time-domain plots. In Figure 8, the current voltage exhibits balanced sinusoidal waveforms (Va, Vb, Vc), the inverter voltage confirms proper functionality, and a single-phase voltage comparison validates phase alignment. The grid voltage, shown in Figure 9, presents synchronized three-phase waveforms oscillating around ±300V, ensuring stability for renewable integration and power distribution. The inverter output currents (Ia, Ib, Ic) in Figure 10 initially display transient peaks due to load variations before stabilizing into balanced sinusoidal waveforms, indicating steady-state operation. These results confirm efficient inverter performance, high-frequency switching, and the system's adaptability to dynamic load conditions. Figure 11 shows the Repeating Sequence Stair1 waveform in magenta, which remains at zero throughout the simulation. This suggests steady-state operation, lack of input, or a misconfigured or uninitialized sequence. The absence of a staircase pattern indicates no triggering occurred. Such waveforms are typically used in digital control, pulse generation, and power electronics applications.

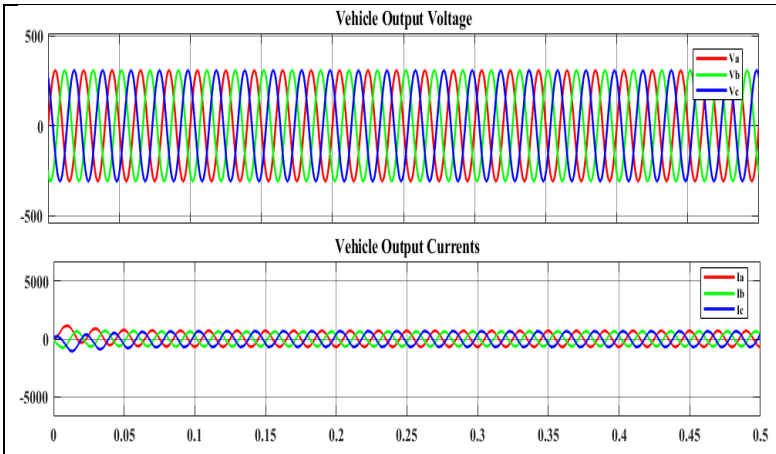

Figure 6 Vehicle output voltage and currents

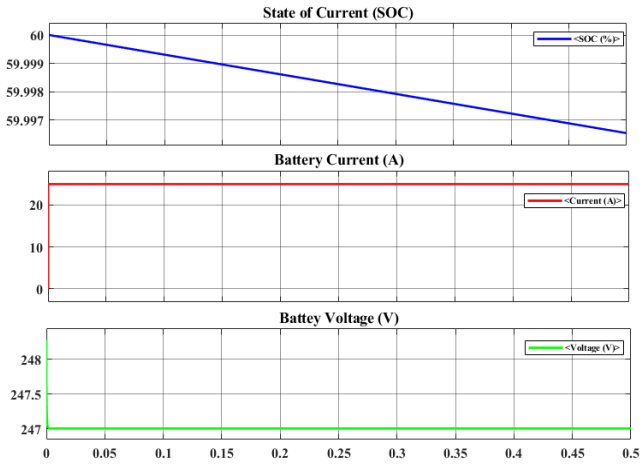

Figure 7 Battery Results

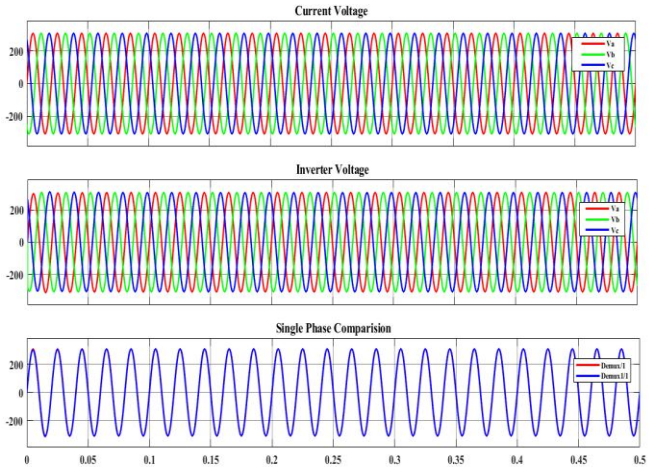

Figure 8 V2G & G2V voltages

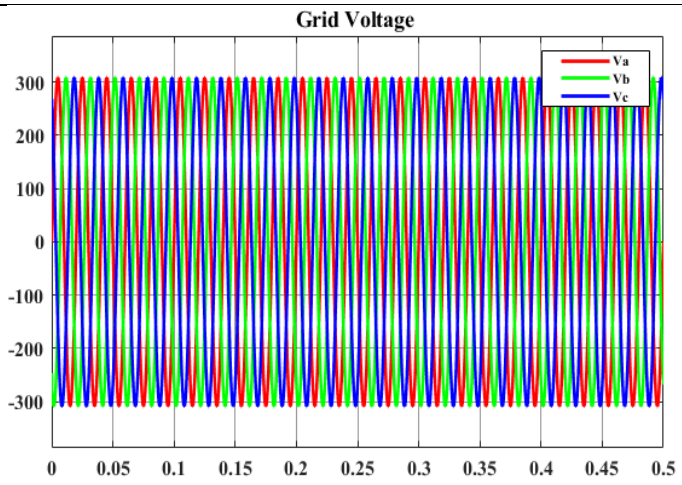

Figure 9 Grid Voltage

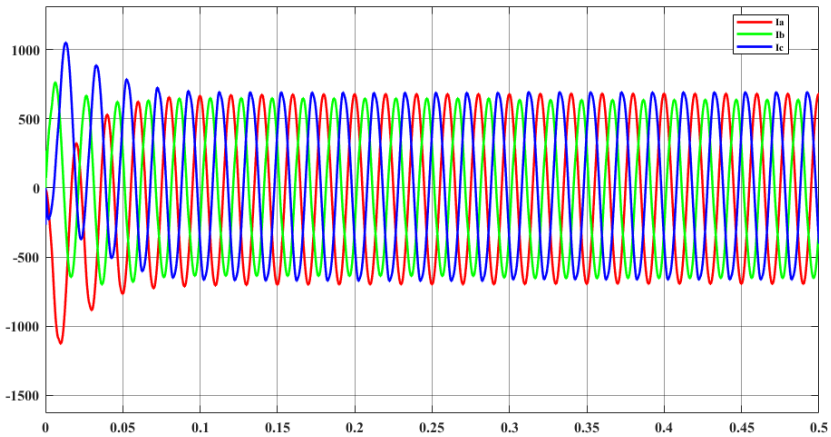

Figure 10 Inverter Currents

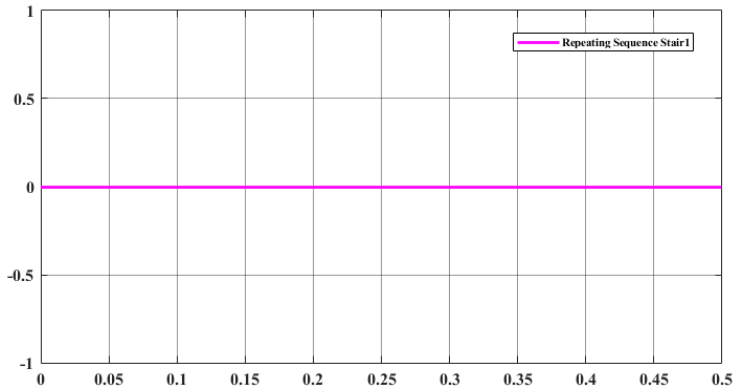

Figure 11 Repeating Sequence Stair Function

4.2 Grid to Vehicle

The G2V operation is demonstrated through a series of figures that collectively validate the charging process and the system's behavior under load. The three-phase sinusoidal waveforms (Va, Vb, and Vc) that make up the vehicle's output voltage, as shown in Figure 12, indicate a high-frequency AC output and validate that the inverter is operating correctly. Due to PWM control, which is often used in inverter-driven systems, the associated current waveforms (Ia, Ib, and Ic) first exhibit a transient condition before settling into a square-wave shape. Figure 13 shows the battery's performance while charging. Active charging is shown by a steady rise in the SOC. While the voltage rapidly increases to a steady level, the battery current first surges high before stabilizing. These actions point to a battery management system that is well-regulated and guarantees reliable functioning throughout the G2V process.The voltage characteristics for both V2G and G2V modes are shown in Figure 14, which offers further information on bidirectional voltage behavior. While the inverter voltage emphasizes the behavior of a single phase, the three-phase voltages preserve balanced sinusoidal waveforms. Maintaining system stability requires evaluating phase consistency and responsiveness during energy transfer, which is made easier by the single-phase comparison at the bottom of the picture. Figure 15 shows the grid voltage state, with symmetrical oscillations of the three-phase waveforms between +500V and -500V. For efficient grid integration during charging operations, a stable grid environment with synchronized phase displacement is reflected in this.Figure 16 analyzes the current flow via the inverter. Curiously, the plot shows no current flowing through phases Ia and Ib, while Ic stays at zero. This suggests that there may be an operational problem, such as an inverter shutdown, a missing load connection, or a control mistake that is inhibiting current production. The Repeating Sequence Stair Function, shown in Figure 17, stays at zero for the duration of the 0.5-second simulation. This implies that the intended step response was not triggered, which might be the result of incorrect sequence logic setup, an inactive signal, or misconfigured simulation.

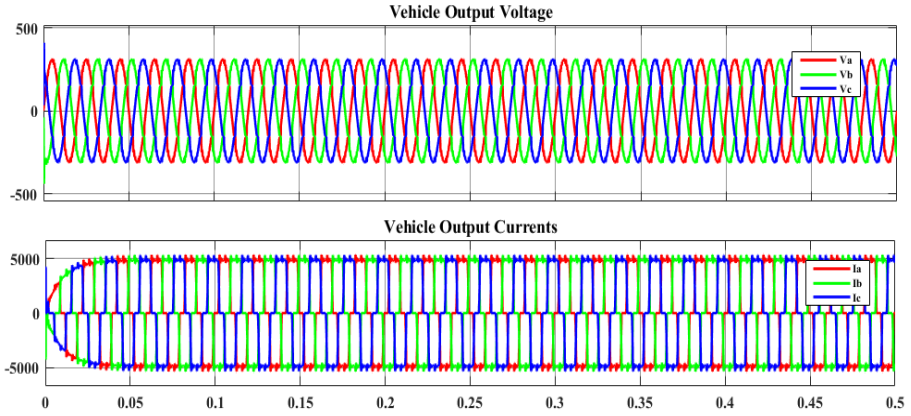

Figure 12 Vehicle output voltage and currents

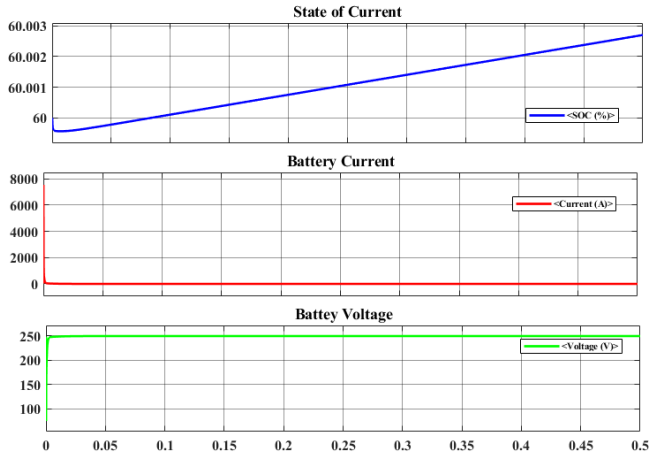

Figure 13Battery Results

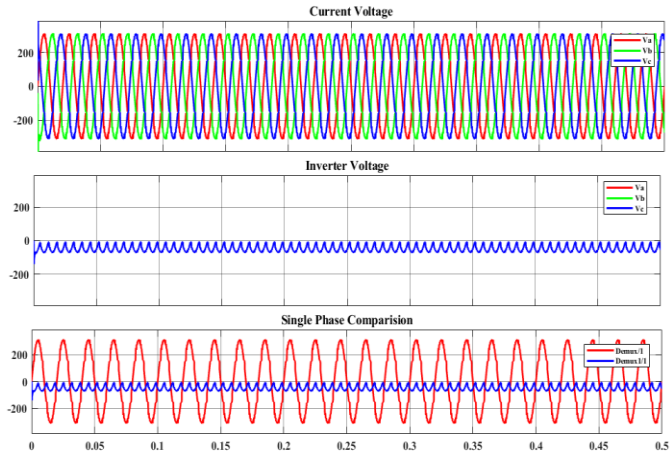

Figure 14V2G & G2V voltages

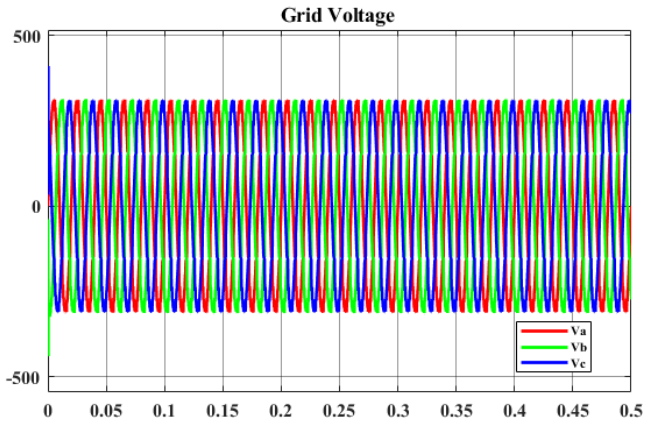

Figure 15Grid Voltage

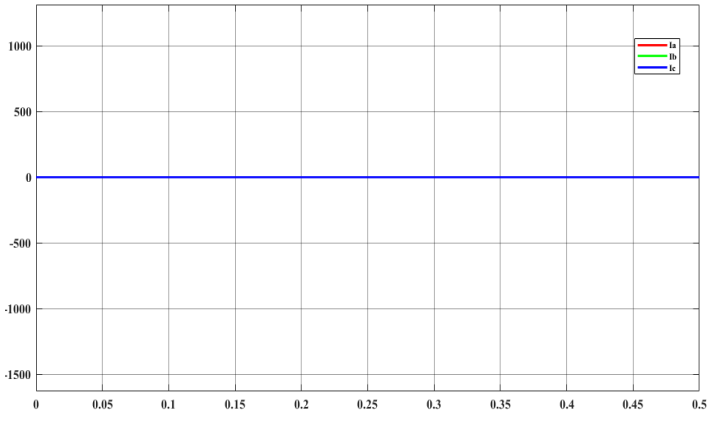

Figure 16 Inverter Currents

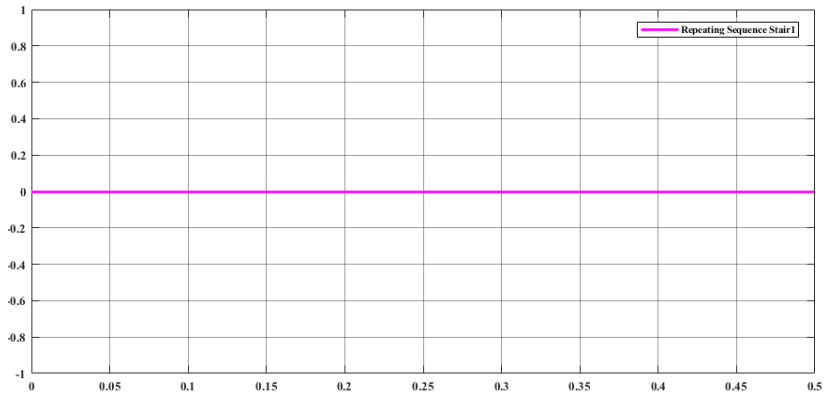

Figure 17 Repeating Sequence Stair Function

4.3 Mixed Method

The system's operational behavior under bidirectional energy flow is demonstrated through a series of waveform analyses, highlighting transitions between G2V and V2G modes. Mode changes are shown by the vehicle output voltage (Va, Vb, and Vc) in Figure 18, which maintains a balanced sinusoidal waveform with notable disturbances at 0.2 and 0.4 seconds. Prior to another transition at 0.4s, the associated output currents (Ia, Ib, and Ic) exhibit initial transients, PWM-controlled patterns, and stabilization. The battery performance in Figure 19 shows the SOC variations (increasing, falling, and recovering) as well as the voltage and current responses that show transient behavior about 0.4s and active charging/discharging.

Figure 20 provides specifics on the voltage characteristics during bidirectional energy transfer. All three subplots show a distinct mode shift with interruptions occurring at 0.4s. Comparisons of phase and inverter voltages show how flexible the system is for G2V and V2G operations. The three-phase grid voltage in Figure 21 is well-balanced and exhibits symmetrical sinusoidal waveforms. It is momentarily disrupted by spikes at 0.2 and 0.4 seconds, which may indicate switching events or grid disturbances.Inverter output currents are shown in Figure 22 as being at zero until 0.2 seconds, after which they change into balanced sinusoidal waveforms and decrease to zero once again at 0.4 seconds. This behavior is indicative of regulated inverter activity and possible system shutdown or switching. Figure 23 shows a step signal (Repeating Sequence Stair1) that presumably acts as a control or triggering signal for system switching events. It changes from 0 to 1 at 0.2s and returns to 0 at 0.4s.

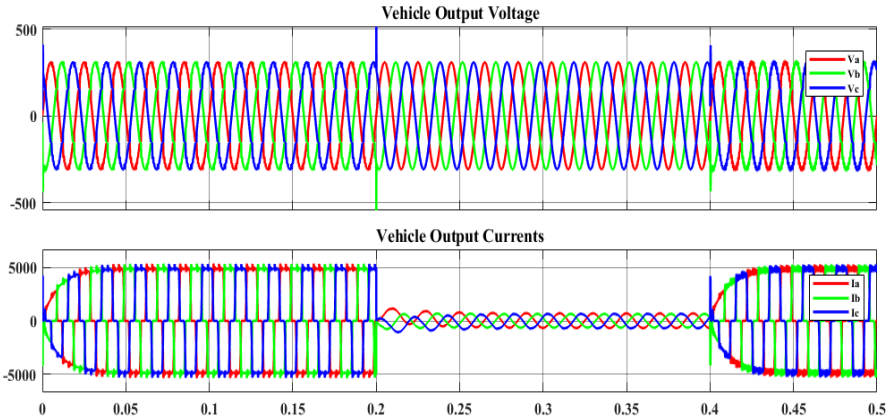

Figure 18Vehicle output voltage and currents

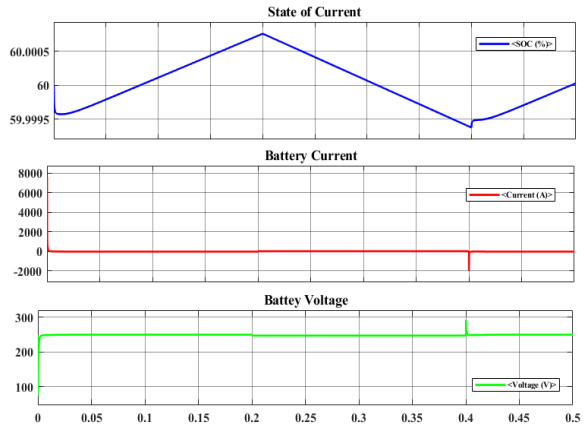

Figure 19Battery Results

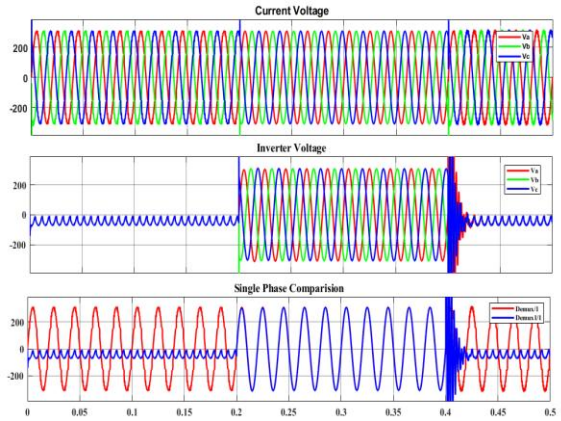

Figure 20V2G & G2V voltages

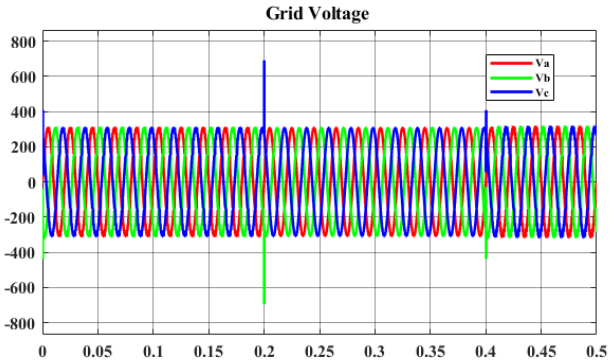

Figure 21 Grid Voltage

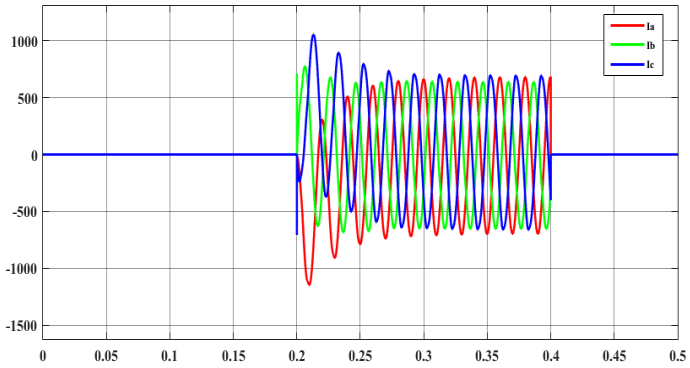

Figure 22Inverter Currents

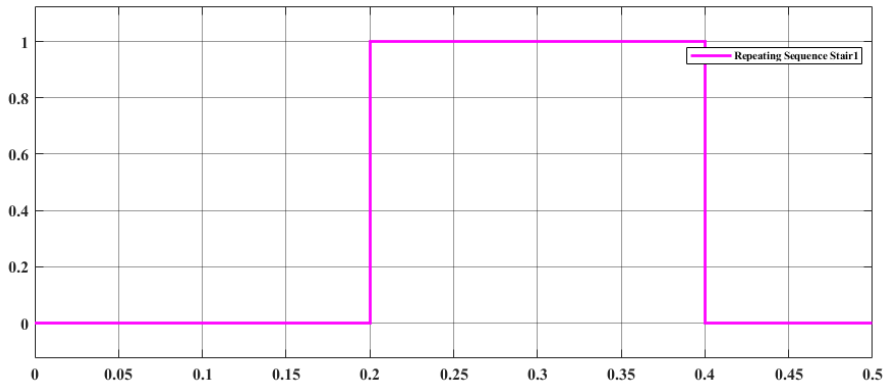

Figure 23 Repeating Sequence Stair Function

4.4 Discussion

The findings provide a thorough understanding of the performance of grid-to-vehicle (G2V) and vehicle-to-grid (V2G) operations, emphasizing the effectiveness, efficiency, and stability of the created energy administration system. The opposite direction power flow is shown by the status of charge (SOC) data, which shows a controlled structure of charging as well as discharging. As the battery is being charged in G2V mode, Figure 16 shows that the state of charge (SOC) rises and diminishes during discharge (V2G mode), hence showcasing the system's proficiency in energy flow management. The battery's current and voltage waveforms corroborate this behavior, demonstrating that an initial high current stabilizes over time, therefore providing appropriate charging characteristics and voltage management.

Figures 17 and 19 show the inverter's voltage and current waveformsdemonstrate the operating dynamics of the power conversion process. The inverter output voltages (Va, Vb, and Vc) exhibit a consistent three-phase sinusoidal waveform, signifying efficient pulse width modulation (PWM) control and synchronization with the grid. Transient spikes occur at certain time intervals (e.g., about 0.2s and 0.4s), indicating mode changes between V2G and G2V operations. The inverter current waveforms exhibit a similar pattern, with the current remaining at zero before to activation, followed by a slow increase and eventual stability, so assuring seamless power supply.

5 Conclusion

This work effectively illustrates the functioning and efficacy Describes a two-way electric vehicle charging batteries system with both Grid-to-Vehicle (G2V) and Vehicle-to-Grid (V2G) capabilities. The suggested MRAC-based control technique effectively regulates battery charging and discharging, facilitating seamless transitions between operating modes. The simulation results confirm that the system sustains balanced three-phase voltage and current waveforms, efficiently controlling SOC and reducing transient fluctuations. The results underscore the significance of grid synchronization and inverter efficacy, validating the viability of using this technology in smart grids and renewable energy applications. Future investigations may include hardware

implementation, real-time control enhancements, as well as the use of sustainable and efficient sources of clean energy.

References

[1] W. Wang and Y. Cheng, "Optimal charging scheduling for electric vehicles considering the impact of renewable energy sources," in *2020 5th Asia Conference on Power and Electrical Engineering (ACPEE)*, IEEE, 2020, pp. 1150–1154.

[2] M. S. Mastoi *et al.*, "An in-depth analysis of electric vehicle charging station infrastructure, policy implications, and future trends," *Energy Reports*, vol. 8, pp. 11504–11529, 2022.

[3] P. Slowik and N. Lutsey, "Expanding the electric vehicle market in US cities," ICCT Washington, DC, USA, 2017.

[4] Y. A. Alhazmi, H. A. Mostafa, and M. M. A. Salama, "Optimal allocation for electric vehicle charging stations using Trip Success Ratio," *Int. J. Electr. Power Energy Syst.*, vol. 91, pp. 101–116, 2017.

[5] M. Clemente, M. P. Fanti, and W. Ukovich, "Smart management of electric vehicles charging operations: The vehicle-to-charging station assignment problem," *IFAC Proc. Vol.*, vol. 47, no. 3, pp. 918–923, 2014.

[6] D. Liu, L. Wang, M. Liu, H. Jia, H. Li, and W. Wang, "Optimal energy storage allocation strategy by coordinating electric vehicles participating in auxiliary service market," *IEEE Access*, vol. 9, pp. 95597–95607, 2021.

[7] J. R. Aguero, E. Takayesu, D. Novosel, and R. Masiello, "Modernizing the grid: Challenges and opportunities for a sustainable future," *IEEE Power Energy Mag.*, vol. 15, no. 3, pp. 74–83, 2017.

[8] G. Buja, M. Bertoluzzo, and C. Fontana, "Reactive power compensation capabilities of V2G-enabled electric vehicles," *IEEE Trans. power Electron.*, vol. 32, no. 12, pp. 9447–9459, 2017.

[9] V. C. Gungor *et al.*, "Smart grid and smart homes: Key players and pilot projects," *IEEE Ind. Electron. Mag.*, vol. 6, no. 4, pp. 18–34, 2012.

[10] A. Jain, K. K. Gupta, S. K. Jain, and P. Bhatnagar, "A bidirectional five-level buck PFC rectifier with wide output range for EV charging application," *IEEE Trans. Power Electron.*, vol. 37, no. 11, pp. 13439–13455, 2022.

[11] P. K. A and H. K. Channi, "A comprehensive review of vehicle-to-grid integration in electric vehicles: Powering the future," 2024.

[12] G. Sun, Y. Zhang, D. Liao, H. Yu, X. Du, and M. Guizani, "Bus-trajectory-based street-centric routing for message delivery in urban vehicular ad hoc networks," *IEEE Trans. Veh. Technol.*, vol. 67, no. 8, pp. 7550–7563, 2018.

[13] K. S. R. Sekhar, M. A. Chaudhari, and V. Khadkikar, "Enhanced hybrid converter topology for PV-grid-EV integration," *IEEE Trans. Energy Convers.*, vol. 38, no. 4, pp. 2634–2646, 2023.

[14] F. Alfaverh, M. Denaï, and Y. Sun, "Optimal vehicle-to-grid control for supplementary frequency regulation using deep reinforcement learning," *Electr. Power Syst. Res.*, vol. 214, p. 108949, 2023.

[15] Q. Sun, H. Xie, X. Liu, F. Niu, and C. Gan, "Multiport PV-assisted electric-drive-reconstructed bidirectional charger with G2V and V2G/V2L functions for SRM drive-based EV application," *IEEE J. Emerg. Sel. Top. Power Electron.*, vol. 11, no. 3, pp. 3398–3408, 2023.

[16] V. Rishishwar, A. Raghuwanshi, and A. Ojha, "Single phase Bi-directional Electric vehicle battery charger with G2V, V2G & V2L Technologies," in *2023 IEEE Renewable Energy and Sustainable E-Mobility Conference (RESEM)*, IEEE, 2023, pp. 1–6.

[17] R. P. Upputuri and B. Subudhi, "A comprehensive review and performance evaluation of bidirectional charger topologies for V2G/G2V operations in EV applications," *IEEE Trans. Transp. Electrif.*, vol. 10, no. 1, pp. 583–595, 2023.

[18] V. K. Manickam and K. Dhayalini, "Hybrid optimized control of bidirectional off-board electric vehicle battery charger integrated with vehicle-to-grid," *J. Energy Storage*, vol. 86, p. 111008, 2024, doi: https://doi.org/10.1016/j.est.2024.111008.

[19] Y. He, B. Venkatesh, and L. Guan, "Optimal scheduling for charging and discharging of electric vehicles," *IEEE Trans. Smart Grid*, vol. 3, no. 3, pp. 1095–1105, 2012.

[20] S. Goel, R. Sharma, and A. K. Rathore, "A review on barrier and challenges of electric vehicle in India and vehicle to grid optimisation," *Transp. Eng.*, vol. 4, p. 100057, 2021.

[21] Z. Hu, K. Zhan, H. Zhang, and Y. Song, "Pricing mechanisms design for guiding electric vehicle charging to fill load valley," *Appl. Energy*, vol. 178, pp. 155–163, 2016.

[22] J. Tan and L. Wang, "Integration of plug-in hybrid electric vehicles into residential distribution grid based on two-layer intelligent optimization," *IEEE Trans. Smart Grid*, vol. 5, no. 4, pp. 1774–1784, 2014.

[23] Z. Tan, P. Yang, and A. Nehorai, "An optimal and distributed demand response strategy with electric vehicles in the smart grid," *IEEE Trans. Smart Grid*, vol. 5, no. 2, pp. 861–869, 2014.

[24] M. S. B. et al. P. K. Maroti, S. Padmanaban, "'The state-of-theart of power electronics converters configurations in electric vehicle technologies,' Power Electronic Devices and Components.," 2022.

[25] H. Neves de Melo, J. P. Trovão, C. Henggeler Antunes, P. G. Pereirinha, and H. M. Jorge, "An outlook of electric vehicle daily use in the framework of an energy management system," *Manag. Environ. Qual. An Int. J.*, vol. 26, no. 4, pp. 588–606, 2015.

[26] U. Sri Anjaneyulu, T. Prathyusha, N. Akhilesh Yadav, V. Prasanth Kumar, and N. Madhava Rao, "A Controllable Bidirectional Battery Charger for Electric Vehicle with Energy Management System," *Int. Res. J. Eng. Technol.*, no. July, 2021.

[27] M. A. Silva, J. P. Trovão, and P. G. Pereirinha, "Implementation of a multiple input DC-DC converter for Electric Vehicle power system," in *Proceedings of the 2011 3rd International Youth Conference on Energetics (IYCE)*, IEEE, 2011, pp. 1–8.